

INTERNATIONAL UNION OF  
PURE AND APPLIED CHEMISTRY

MACROMOLECULAR DIVISION

THE EFFECT OF MOLECULAR ORIENTATION  
ON THE MECHANICAL PROPERTIES OF  
POLYSTYRENE

*A Report of the IUPAC Working Party on "Structure and Properties of Commercial Polymers", being the first in a Programme of Study on Orientation in Polymers*

*Prepared for publication and presented at the IUPAC International Symposium on Macromolecules, Aberdeen, 10-14 September 1973*

Prepared for publication by

T. T. JONES

Monsanto Limited, Rideal Laboratories, Newport, Gwent, NPT OXF, UK

PERGAMON PRESS  
OXFORD · NEW YORK · PARIS · FRANKFURT

## MACROMOLECULAR DIVISION

# THE EFFECT OF MOLECULAR ORIENTATION ON THE MECHANICAL PROPERTIES OF POLYSTYRENE

**Abstract**—Oriented sheets of two commercial homopolystyrenes differing in molecular weight, rheological and glass transition temperature properties have been prepared by sheet extrusion and drawing.

The properties of the resulting sheets have been studied at seven different laboratories in Europe.

The degree of orientation, irrespective of how it is achieved, is defined in terms of the birefringence which is proportional to the maximum shrinkage stress through the stress optical coefficient, and to a sonic modulus function. The nominal draw ratio and the length reversion ratio are not unequivocal estimates of the degree of orientation.

The orientation stress can be divided into two parts, the first is associated with Hookean elasticity and the other with rubber-like elasticity. It is the deformation due to this latter part that gives rise largely to the properties of the oriented solid polymers.

From the value of the stress optical coefficient and the relation between maximum shrinkage stress and length reversion ratio estimates of the size of the random link and of the effect of temperature of orientation and strain rate on the degree of chain entanglement are obtained.

Tensile properties including rupture stress, rupture strain and rupture energy have been determined over a wide range of strain rates for the various degrees of orientation. Increasing orientation generally improved rupture stress as also did strain rate but as orientation increased and rupture took place by yielding the rupture stress tended to fall. The rupture strain would then tend to increase as also would rupture energy. These effects, as well as maxima observed in rupture strain with time to rupture are believed due to the secondary or  $\beta$  relaxation process of polystyrene. The effect of angle to draw direction on tensile properties is examined.

In addition to estimates of the sonic modulus the stress relaxation modulus at increasing times was also investigated.

Other properties examined have been the variation of impact strength with orientation and angle to draw direction and also environmental stress cracking.

### CONTENTS

1. Introduction	41
2. Section (a) Characterisation of the Raw Materials	42
2.1 Molecular Weight Characterisation	42
2.2 Glass Transition Temperature, $T_g$	42
2.3 Melt Rheology	42
2.4 Conclusions	42
3. Section (b) Preparation of Oriented Sheet Materials	43
4. Section (c) The Degree of Orientation	43
4.1 The Length Reversion Ratio	43
4.2 Birefringence	44
4.2.1 Birefringence and nominal draw ratio	44
4.2.2 Variation of birefringence with depth within sheet	44
4.2.3 Birefringence and length reversion ratio	44
4.3 The Orientation Parameter	45
4.3.1 Birefringence and orientation stress	46
4.3.2 Birefringence, orientation stress, shrinkage stress and stress relaxation	46
4.3.3 Birefringence and sonic modulus	49
4.4 Conclusions	49
5. Section (d) Some Properties of the Oriented Sheets	49
5.1 Tensile Properties	49
5.1.1 The estimation of strain rate, $\dot{\epsilon}$	49
5.1.2 The estimation of specific rupture energy, $W_r$	49
5.1.3 The variation of rupture stress with strain rate and orientation	50
5.1.4 The variation of rupture strain with strain rate and orientation	50
5.1.5 The variation of specific rupture energy, $W_r$ , with strain rate and orientation	50
5.1.6 Variation of rupture strain with time to rupture	51
5.1.7 The time dependent Young's Modulus of Elasticity, $E(t)$ , and the relaxation spectrum $H(\ln \tau)$	52
5.1.8 The effect of temperature on tensile properties	52
5.2 Impact Strength	53
5.3 Environmental Stress Cracking	53
6. Summary and Conclusions	54
References	56
Appendix	57

### 1. INTRODUCTION

This paper is one of a number of papers resulting from the work of a Working Party set up in 1963 by the High Polymer Section of the International Union of Pure and Applied Chemistry to study "The Relationship of

Performance Characteristics to Basic Parameters of Polymers".

So far the working party has published a variety of papers dealing with studies carried out exclusively on commercial polymers which have been selected because

of their technological importance and their ready availability in large quantities.<sup>1-5</sup> More recently therefore the purpose of the working party, which is now within the Macromolecular Division of I.U.P.A.C. has been restated as a study of "The Structure and Properties of Commercial Polymers".

The present paper is the first of a series of papers on the subject of the effects of orientation on the properties of polymers. It is recognised that a softened polymer subjected to any mechanical operation such as compression or injection moulding, extrusion, vacuum forming, film blowing etc., becomes oriented, and that a completely relaxed solid polymer is rarely met with in practice. The study of the effects of orientation on the properties of polymers is therefore an important one and the working party agreed that such a study on as wide a variety of commercial polymers as possible was most worthwhile.

The present paper deals with such studies on atactic polystyrene, a simple, amorphous, non toughened, non crystalline polymer available in sufficient quantities to allow the preparation of the required oriented sheets and to supply the raw material as required.

The participants in this study were as follows:

- I ○ Badische Anilin and Soda-Fabrik A. G., Ludwigs-hafen (Rhein), West Germany.
- II △ Farbwerke Hoechst A. G., Frankfurt (Main), West Germany.
- III □ Monsanto Limited, 10-18 Victoria Street, London S.W.1H. 0NQ. Some of the work of Monsanto was carried out in collaboration with the Institute of Polymer Technology, University of Loughborough. This will be referred to as III.L.
- IV ▽ Montecatini Edison S.p.A., Bollate, Milan, Italy.
- V Produits Chimiques Péchiney-Saint-Gobain, Antony, France.
- VI ◇ Solvay and Cie, Laboratoire Central, Brussels, Belgium.
- VII × Technical University, Prague, C.S.S.R.

Each participant will be referred to henceforth by the Roman numerals, and experimental points on all figures will be designated by the symbols given. Two commercial polystyrenes in general use, differing in molecular weight and rheological properties and available in large quantity were supplied by Participant III.

The polystyrenes, designated PSA and PSB, were available as moulding pellets or as sheets which III prepared by sheet extrusion in the unoriented form or as oriented sheets at three nominal draw ratios or degrees of orientation. The studies are divided into four well defined sections, namely (a) Characterisation of the raw materials, (b) Preparation of oriented sheet materials, (c) The degree of orientation, and (d) Some properties of the oriented sheets.

## 2. SECTION (a) CHARACTERISATION OF THE RAW MATERIALS

The polystyrenes PSA and PSB were characterised in terms of molecular weight, glass transition temperature as determined by a torsion pendulum and rheological properties.

### 2.1 Molecular weight characterisation

Participants II, III, IV and V determined number and weight average molecular weights of the pellets from molecular weight distribution obtained by gel permeation

Chromatography using tetrahydrofuran as solvent at temperatures of 23°, 25° and 45°C. Participant III also used toluene as solvent at 80°C. III and V also determined the molecular weight characteristics of sheet material.

In addition, V determined the intrinsic viscosity in tetrahydrofuran at 25°C,  $[\eta]_{\text{exp}}$ , and compared it with the value calculated,  $[\eta]_{\text{calc}}$ , from the viscosity average molecular weight  $\bar{M}_v$  obtained from the distribution curve by using the appropriate relations,<sup>6</sup> namely

$$[\eta]_{\text{calc}} = 1.17 \times 10^{-2} \bar{M}_v^{0.725}$$

where

$$\bar{M}_v = \left\{ \frac{\sum w_i M_i^{0.725}}{\sum w_i} \right\}^{1/0.725}$$

Table 1 summarises the results obtained.

It is seen from these results that both  $\bar{M}_n$  and  $\bar{M}_w$  are higher for PSB than for PSA while the ratio  $\bar{M}_w/\bar{M}_n$  is not as large. The higher  $\bar{M}_w/\bar{M}_n$  ratio for PSA is due to the presence of relatively more low molecular weight material. In all cases the  $\bar{M}_v$  values lie closer to  $\bar{M}_w$  than  $\bar{M}_n$ .

The effect of sheet extrusion is to decrease both  $\bar{M}_n$  and  $\bar{M}_w$  the former being about 10-15% lower and the latter about 3-6%. This is caused by degradation and results in a greater polydispersity.

### 2.2 Glass transition temperature, $T_g$

Glass transition temperatures for unoriented PSA and PSB were determined by I and VI by means of torsion pendula at a frequency of about 1 Hz. Estimates of  $T_g$  as given by the position of the  $\tan \delta$  loss peak were not in good agreement the values found by I being 99°C and 106°C for PSA and PSB respectively and those found by VI being 107°C and 112°C respectively. VII also carried out torsion pendulum studies at about 1 Hz but did not investigate the position of the damping peaks. However  $\tan \delta$  had a value of 0.1 at temperatures of 87°C and 98°C for PSA and PSB respectively. It is seen that values of  $T_g$  at 1 Hz are not well defined but they do differ for the two polymers by about 6 or 7°C, PSB having the higher  $T_g$ . Participant IV using a differential scanning calorimeter at a heating rate of 8°C/min found values for  $T_g$  of 93°C and 100°C for PSA and PSB respectively. This confirms that there is a difference in  $T_g$  of about 7°C for the two polymers.

### 2.3 Melt rheology

Participants III and IV determined the melt viscosity of the two polymers at 200°C by means of capillary rheometers. A total range of uncorrected shear rates from 1 to 5000  $\text{sec}^{-1}$  was covered. At 1  $\text{sec}^{-1}$  PSB had an apparent melt viscosity of about  $1.4 \times 10^5$  P which was over twice as much as for PSA while at 5000  $\text{sec}^{-1}$  the viscosity of PSB had dropped to about  $6.6 \times 10^2$  P which was about 30% greater than for PSA.

### 2.4 Conclusions

The polystyrenes submitted for study differ quite significantly in their molecular weight, molecular weight distribution, glass transition temperatures and melt viscosities.

Attention will be paid to the part played by these differences in influencing the process of orientation and the ultimate properties of the oriented polymers.

Table 1. Summary of molecular weight determinations by G.P.C. and intrinsic viscosity determinations, for PSA and PSB pellets and sheets

Material	Participants	Mean of number average molecular weight ( $\bar{M}_n$ )	Standard deviation of $\bar{M}_n$ (%)	Mean of weight average molecular weight ( $\bar{M}_w$ )	Standard deviation of $\bar{M}_w$ (%)	Mean ratio $\bar{M}_w/\bar{M}_n$	Intrinsic viscosity in tetrahydrofuran at 25°C (Participant V) $[\eta]_{exp}$ (ml/g)	Viscosity average molecular weight from distribution curve ( $\bar{M}_v$ )	Intrinsic viscosity from $\bar{M}_v$ $[\eta]_{calc}$ (ml/g)
PSA pellets	II, III, IV and V	67,770	18.8	237,500	4.7	3.6	82.7	207,690	83.8
PSA sheet	III and V	62,430	15.8	232,000	7.8	3.76	76.8	187,400	77.8
PSB pellets	II, III, IV and V	114,960	24.1	311,400	6.1	2.85	103.8	270,670	101.5
PSB sheet	III and V	101,130	25.1	293,000	8.5	3.04	88.8	237,800	92.4

### 3. SECTION (b) PREPARATION OF ORIENTED SHEET MATERIALS

The preparation of sheet material of varying nominal draw ratios was conducted on a continuous basis by means of sheet extrusion followed by drawing of the extruded sheet to varying degrees. In addition to nominally undrawn sheet the nominal draw ratios attained were 1.5:1, 2.6:1, and 3.9:1, and all sheets were approximately 3 mm thick except some required by I at a thickness of 0.5 mm.

The system used is illustrated schematically in Fig. 1. It consisted essentially of an extruder giving a constant output of molten polymer sheet through a 14 in. slit die having an adjustable gap. The sheet then entered between the two top rolls of a triple calender rolls which were adjusted to just nip the sheet on entry. The sheet then passed between the second and third rolls and eventually to the haul-off rolls after passing between two heaters to maintain the temperature of the sheet during the drawing operation. This was effected by running the haul-off rolls at the same speed as the triple rolls or at any desired faster speed, the ratio of the two speeds being kept constant. This ratio is termed the nominal draw ratio.

### 4. SECTION (c) THE DEGREE OF ORIENTATION

In any study of orientation of polymers a measure of the degree or extent of orientation is essential since the ultimate properties of the oriented polymer must be described in terms of the orientation present.

In the case of cross-linked rubbers the extension ratio  $\lambda$  is a measure of orientation where  $\lambda$  is the ratio of the extended length  $l$  to the original length  $l_0$ .

$$\text{i.e. } \lambda = l/l_0.$$

The oriented PSA and PSB sheets were prepared while the materials were in the softened rubbery state. But since the materials were not cross-linked and since the conditions for producing the sheets differ slightly within any one nominal draw ratio and quite significantly from one nominal draw ratio to the next the degree of extension or draw ratio imparted to the material was merely a convenient way of describing the sheets produced. The degree of contraction or length reversion ratio on annealing the oriented material above its  $T_g$  would be a closer approximation to the extension ratio present in the material in the solid state. The length reversion ratio is therefore one measure of orientation which has been examined.

A further measure of orientation is that of birefringence. Polystyrene is an amorphous polymer which exhibits considerable birefringence on stretching in the rubbery state and this is uncomplicated by crystallinity. The birefringence of a completely oriented polystyrene can be estimated theoretically and so the degree of orientation can be defined in terms of the birefringence. The stress required to orient the polymer chains is connected with the birefringence through the stress optical coefficient. This stress, as given by the maximum shrinkage stress, has also been investigated as a measure of degree of orientation.

Finally the extension modulus of oriented amorphous polymers is a function of the degree of orientation. This relationship was also examined.

#### 4.1 The length reversion ratio

The degree of contraction of length that takes place when an oriented specimen is kept at a high enough temperature for a sufficient time so as to lose its orientation and attain a completely relaxed state is termed the length reversion ratio, LRR. If  $l_1$  is the initial length along the

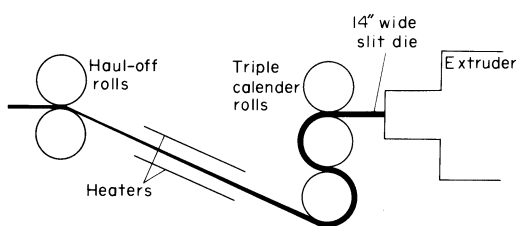


Fig. 1. Schematic diagram of extruded oriented sheet preparation.

In order to maintain a constant final thickness of sheet it was necessary to build up varying thicknesses of polymer at the triple roll entry position. This was attained by both speeding up the extruder output and slowing down the triple roll speed until the desired thickness was obtained. This thicker polymer sheet, on drawing between the triple rolls and the haul-off rolls, yielded the desired thickness of oriented sheet. The final sheet material was cut into lengths of about 1 m the smallest width at the highest draw ratio being about 150 mm and that for the undrawn material about 300 mm.

orientation direction and  $l_2$  the final relaxed length, then the length reversion ratio  $LRR = l_1/l_2$ .

Conditions of annealing differed widely as each participant endeavoured to attain the maximum reversion possible. Figure 2 shows the relationship between LRR and nominal draw ratio NDR, for PSA and PSB respectively, the participants and conditions of annealing being also indicated. Apart from the work carried out by II on 0.015 mm thick microtomed samples, all other reversions were carried out on 3 mm thick samples cut from the sheets supplied. Only experimental points for PSA are given.

There is a wide spread of points for any one nominal draw ratio and the curves have been drawn through positions of highest density of points. It is seen from these plots that LRR is greater than NDR for both polymers up to NDR about 3.7 since the curves lie above the line drawn at 45°. This is due to slight orientation imparted to the sheet between the die and top two calender rolls. The trend to slightly lower values of LRR at the highest NDR is due to relaxation caused by the higher temperature of the sheet required in order not to overload the machine.

The lack of agreement of LRR amongst themselves may reflect the difficulty of making oriented sheet of constant thickness and constant orientation rather than any difficulties in attaining a reliable estimate of LRR. Thus a number of participants reported results obtaining after ensuring that the LRR did not vary after keeping beyond a certain time at the temperature and in the medium chosen. It is felt however that relaxation kinetics requires further study. Evidence of some biaxial orientation was obtained by III since the width and thickness expansion ratios  $w_2/w_1$  and  $t_2/t_1$  were not equal, but their product was not unduly different from LRR indicating no change in volume on drawing. Slight width-wise orientation was indicated since  $w_2/w_1$  was always a little less than  $t_2/t_1$ .

#### 4.2 Birefringence

Participants I, II and III measured the birefringence of the oriented sheets,  $\Delta n_{zy}$ , while II also measured the variation of birefringence with depth from the surface of

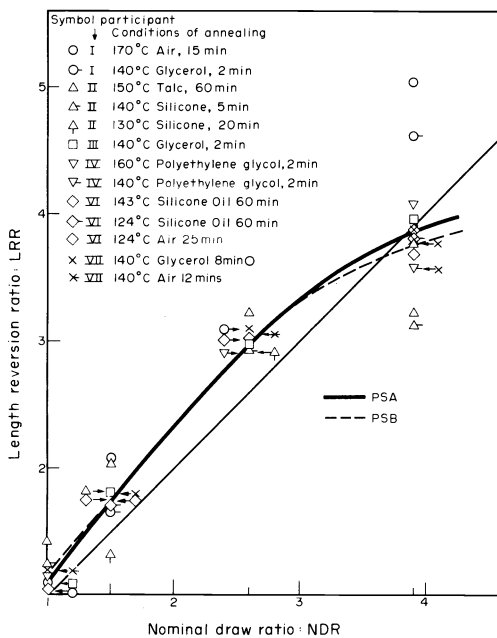


Fig. 2. Plots of length reversion ratio against nominal draw ratio for PSA and PSB. Experimental points for PSA only.

the sheet in the orientation direction,  $\Delta n_{yx}$ , and also in a direction along the width,  $\Delta n_{zx}$ , the birefringence being defined in terms of the following cartesian co-ordinates: z along the draw direction; y, along the width of the sheet and x, normal to the plane of the sheet.

**4.2.1 Birefringence and nominal draw ratio.** In the same way as length reversion ratio has been compared with nominal draw ratio the way in which the birefringence  $\Delta n_{zy}$  varies with NDR may also be observed. Figure 3 shows this relationship for PSA and PSB the experimental points for PSA only being plotted.

Again no linear relationship exists between NDR and birefringence and this further shows that sheets drawn to the same NDR do in fact differ significantly in birefringence. The plots are similar in shape to those for LRR against NDR but PSB is seen to be decidedly higher in birefringence than PSA for the same NDR.

Since the conditions of drawing, particularly the temperature and time of drawing, differed for each NDR, and even for any one NDR, it is not surprising that the above rather wide spread of birefringence exists.

**4.2.2 Variation of birefringence with depth within sheet.** In general the birefringence values were not constant at different depths. Whereas the mean of all  $\Delta n_{zx}$  values at different depths was not greatly different from the value for  $\Delta n_{zy}$ , the variation with depth showed that the material had relaxed to varying degrees during drawing the greatest relaxation taking place within the sheet and nearer the lower surface which retained heat better.

For a uniaxially drawn material  $\Delta n_{yx}$  should be zero. However, small but significant values were observed for all samples tested which undoubtedly indicates some biaxial orientation, the sign of the birefringence indicating slight width-wise orientation in agreement with the width expansion ratio evidence.

Figure 4 gives an example of how birefringence varies with depth. It is for a sample of PSA sheet at NDR = 2.6.

**4.2.3 Birefringence and length reversion ratio.** It is now evident that NDR cannot be used as a measure of orientation. The way in which birefringence varies with length reversion ratio however is more reliable. Figure 5 shows this relationship for PSA and PSB the experimental points for PSA only being shown.

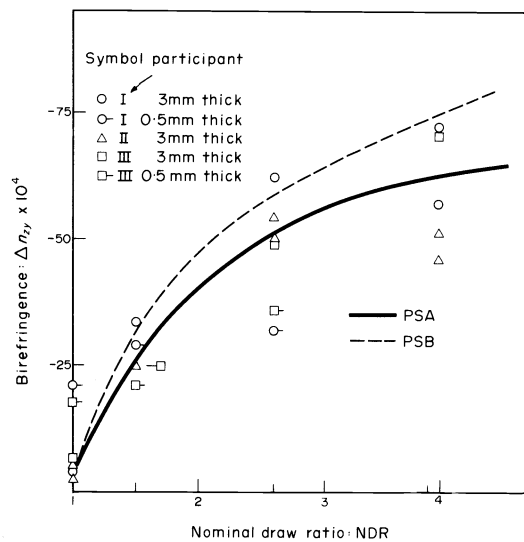


Fig. 3. Plots of birefringence against nominal draw ratio for PSA and PSB. Experimental points for PSA only.

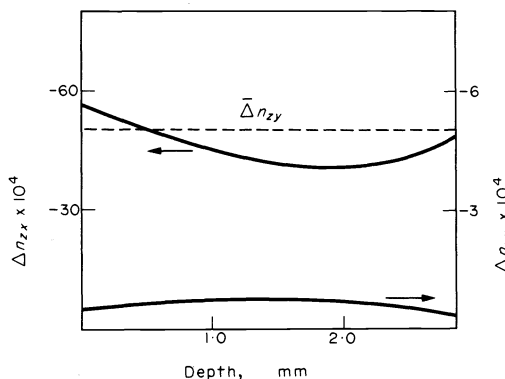


Fig. 4. Variation of birefringence with depth for a sample of PSA sheet, NDR = 2.6.

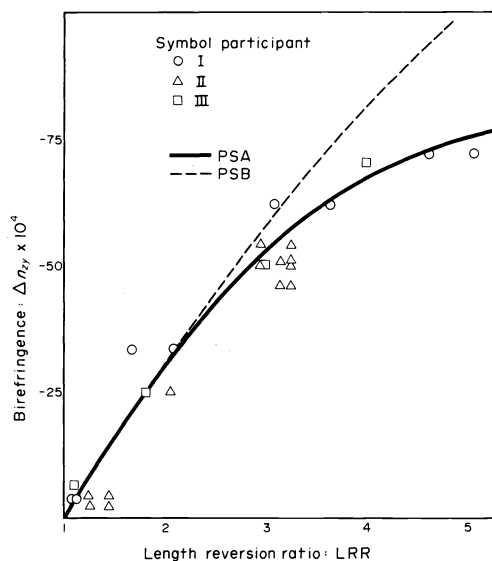


Fig. 5. Plots of birefringence against length reversion ratio for PSA and PSB. Experimental points for PSA only.

While the scatter of points is still rather high there is a better relationship between birefringence and LRR for both polymers, with PSB having a greater birefringence than PSA for the same LRR particularly at high values of LRR. On the basis of rubber elasticity theory however, e.g. see Treloar,<sup>7</sup> the shape of the plots is incorrect in that birefringence should be a function of  $[(LRR)^2 - (LRR)^{-1}]$  i.e. the birefringence should increase more rapidly than LRR. This is true however for a cross-linked rubber having a fixed degree of cross-linking. The polystyrene melts, a little above their  $T_g$ , are not true rubbers but are in a rubbery state in virtue of temporary entanglements which are both temperature and time dependent. Since the sheets were subjected to different strain rates and temperatures during orientation it is not to be expected that  $\Delta n_{zy}$  would be a function of  $[(LRR)^2 - (LRR)^{-1}]$ . The more highly oriented sheets would be drawn at a higher temperature since the thickness of hot polymer would be greater and so retain its heat longer. This would reduce the degree of temporary chain entanglement and so the birefringence. The relationship between birefringence and LRR is thus purely arbitrary and a direct result of the conditions of temperature and strain rates required to produce the sheets.

### 4.3 The orientation parameter

It is appropriate at this point to consider how orientation can be stated in quantitative terms varying from zero orientation to 100% orientation. It is not difficult to visualise these two extremes. A completely unoriented system will be composed of a random mixture of chain molecules while 100% orientation would be these chains in the fully extended state and aligned parallel to each other.

If the chains are considered as composed of statistical segments or links joined at random, then in the unoriented state these links will be at angles  $\theta_1, \theta_2, \theta_3, \dots$  to any direction along which orientation will take place. After orientation these same links will be at angles  $\theta'_1, \theta'_2, \theta'_3, \dots$  to the direction of orientation.

It can be shown that the mean value of  $\overline{\cos^2\theta}$  for a completely random system of links is  $1/3$ , while for a completely oriented system  $\theta'_1 = \theta'_2 = \theta'_3 = \dots = 0$  and so the mean value of  $\overline{\cos^2\theta} = 1$ . Hermans<sup>8</sup> has defined an orientation factor  $\alpha = (3\overline{\cos^2\theta} - 1)/2$ , which is termed the total molecular orientation and which varies from zero for a completely random system to 1 for 100% orientation. In the case of non-crystalline polymers this factor is also equal to the optical orientation factor  $f = \Delta n / (n_\alpha - n_\beta)$  where  $n_\alpha$  is the refractive index along a molecular segment and  $n_\beta$  that at right angles i.e.  $n_\alpha - n_\beta$  is the birefringence of a completely oriented system.

Moseley<sup>9</sup> showed that the total molecular orientation  $\alpha$  is also given by  $\alpha = 1 - E_u/E$ , where  $E_u$  is the sonic modulus of the unoriented system and  $E$  the sonic modulus along the direction of orientation.

Also Morgan,<sup>10</sup> basing his work on that of De Vries,<sup>11</sup> confirmed the expected linear correlation between the birefringence and the orientation factor  $\alpha$ , measured by sonic modulus.

Further, the kinetic theory of rubber-like elasticity,<sup>7</sup> leads to an expression for the birefringence of an oriented cross-linked rubber namely

$$\Delta n = \frac{2\pi(\bar{n}^2 + 2)^2}{45\bar{n}} \cdot N(\alpha_1 - \alpha_2)(\lambda^2 - \lambda^{-1})$$

where  $\bar{n}$  is the mean refractive index,  $N$  is the number of chains per unit volume,  $\alpha_1$  and  $\alpha_2$  are the polarizabilities of the random molecular segment along and transverse to its length and  $\lambda$  is the extension ratio.

The same theory connects the stress  $\sigma$  produced during uniaxial extension with  $\lambda$  by the expression

$$\sigma = NkT(\lambda^2 - \lambda^{-1})$$

where  $\sigma$  is the stress on the strained cross-section,  $k$  is Boltzmann's constant and  $T$  the absolute temperature.

The ratio of  $\Delta n$  to  $\sigma$  is the stress optical coefficient, SOC. Hence

$$\frac{\Delta n}{\sigma} = \text{SOC} = \frac{2\pi(\bar{n}^2 + 2)^2}{45kT\bar{n}}(\alpha_1 - \alpha_2),$$

an expression which is independent of the extension ratio and the degree of cross-linking and which requires birefringence to be a linear function of orientation stress at constant temperature.

It is therefore seen that birefringence, the sonic modulus function  $(1 - E_u/E)$  and orientation stress are direct measures of molecular orientation and studies of each of these properties were conducted by a number of participants.

**4.3.1 Birefringence and orientation stress.** The actual stress required to prepare oriented PSA and PSB sheets was not measured but within the oriented sheet is a latent stress which manifests itself on heating the sheet above  $T_g$ . This is known as the shrinkage stress and was studied by participants I, III, III L and IV. It is this stress that will be expected to be linearly related to birefringence. I studied the shrinkage stress by heating in air specially prepared 0.5 mm thick specimens, 10 mm wide, held in an Instron tensile testing machine between clamps 100 mm apart and connected to a load cell. As the temperature was increased at a rate of 3°C/min the shrinkage stress developed and attained a maximum  $\sigma_{smax}$  at about the  $T_g$  and then subsided as the specimen relaxed on further heating.

IV studied the shrinkage stress using 3 mm thick samples cut from the oriented sheets, 10 mm wide and 50 mm gauge length. The sample was clamped at the base of a rigid transportable frame, the upper clamp being connected by means of a steel wire to a load cell at the top of the frame. The clamped sample was immersed in a thermostated polyethylene glycol bath at 70°C for 10 min and then heated at 2°C/min to 150°C. The shrinkage stress developed in the same way as observed by I. IV also carried out experiments similar to I in an Instron machine heating at 5°C/min, and also measured  $\sigma_{smax}$  by suddenly immersing the clamped specimen in a polyethylene glycol bath at 150°C. In all these experiments the same value of  $\sigma_{smax}$  was obtained showing that it is not affected by the rates of heating used.

Participant III prepared specially oriented sheets of PSB in a Brückner Biaxial Orientation Machine at temperatures varying from 115 to 180°C. The same draw ratio was used at all temperatures namely about 3:1 the starting material being 30 cm square nominally undrawn PSB sheet drawn at a speed of 63.5 cm min<sup>-1</sup>. The resulting sheets decreased in birefringence as the temperature of orientation was increased. The  $\sigma_{smax}$  was determined in an Instron tensile testing machine by very rapid heating of a 1.25 cm wide, 12.5 cm long sample, placed between parallel plate radiant heaters 3.2 cm long and 6 mm apart maintained at 350°C.

Participant I also determined the decrease in  $\sigma_{smax}$  for an oriented specimen of NDR = 3.9 after annealing at a constant length at 105°C for about 25 min and compared it with the decrease in birefringence.

Finally participant III L prepared oriented specimens of PSA and PSB by drawing under controlled conditions of strain rate,  $0.33 \times 10^{-2}$  to  $8.33 \times 10^{-2}$  sec<sup>-1</sup>, and temperature 100–115°C. The  $\sigma_{smax}$  of these oriented specimens were also measured relative to their birefringences.

The results of all the above work are collected in Fig. 6 where birefringence is plotted against  $\sigma_{smax}$  for both PSA and PSB. There is essentially no difference between the two polymers. The points are seen to lie reasonably on a linear plot through the origin as was expected and the slope of this line gives the stress optical coefficient, SOC. The value so obtained is -5200 Brewsters where 1 Brewster =  $10^{-6}$  mm<sup>2</sup>/N. This value is in good agreement with those reported in the literature for polystyrene in the rubbery state.<sup>12-14</sup>

**4.3.2 Birefringence, orientation stress, shrinkage stress and stress relaxation.** Whereas the actual stress required to produce the oriented sheets of PSA and PSB at various NDR's was not measured participant III L did devise experiments in which the orientation stress as well as the shrinkage stress was measured in carefully controlled experiments conducted at different strain rates and at different temperatures. Carefully moulded, annealed and relaxed PSA and PSB sheets were prepared and tensile test

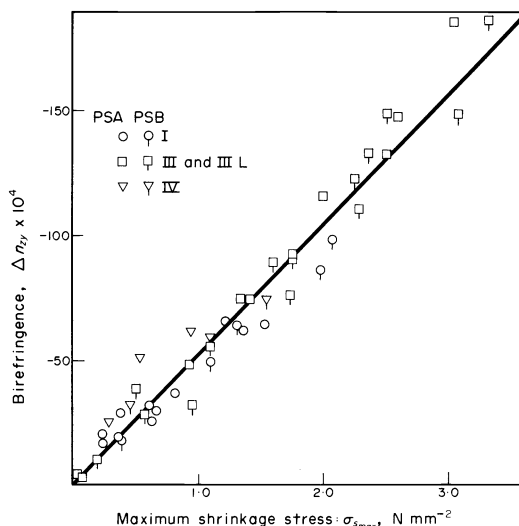


Fig. 6. Plot of birefringence against maximum shrinkage stress of oriented samples of PSA and PSB drawn under different conditions of strain rate and temperature. Birefringence measured on specimens that were then used for shrinkage stress test.

pieces 14.5 cm long and 2 cm wide with a reduced width of 1 cm over a length of 10.5 cm were drawn to a constant draw ratio of approximately 3.5 at temperatures between 100 and 115°C and strain rates  $0.33 \times 10^{-2}$  sec<sup>-1</sup> to  $8.33 \times 10^{-2}$  sec<sup>-1</sup>. One experiment was also conducted at 133°C and the lowest strain rate. The maximum stress  $\sigma_{smax}$  after attaining the fixed final strain was recorded and the specimen was then immediately cooled by a burst of CO<sub>2</sub> coolant. The birefringence and maximum shrinkage stress of the resulting specimens were measured and have been included in the results plotted on Fig. 6. In addition the length reversion ratio and the width and thickness expansion ratios were also measured.

It was noticed that the apparent stress optical coefficient obtained from the ratio of birefringence to maximum orientation stress was always smaller than the one obtained using the maximum shrinkage stress namely the stress optical coefficient already reported. The apparent SOC approached this highest value the higher the temperature and lower the strain rate. Also, owing to the difference in molecular weight and viscosities, PSB at a temperature 5°C higher than PSA behaved in much the same way as PSA. These results are shown in Fig. 7.

The maximum orientation stress is evidently not attained in a maximum shrinkage stress determination although the birefringence still remains proportional to the latter. The orientation stress must therefore contain a portion which is lost or relaxed quickly between the cooling of the oriented specimen and the subsequent determination of  $\sigma_{smax}$ .

It is well known that the SOC of polystyrene depends upon whether it is in the glassy or rubbery state e.g. see Wilkes and Stein.<sup>15</sup> In the vicinity of  $T_g$  it is therefore not unexpected that the polymer can have an apparent SOC which lies somewhere between the values for the rubbery state and the glassy state.

The values of the SOC in the rubbery state are in the region of -5000 Brewsters as already indicated. The negative value is caused by chain orientation along the drawing direction causing the phenyl groups, which are more polarizable than the chain itself, to be disposed in a direction tending to be perpendicular to the drawing

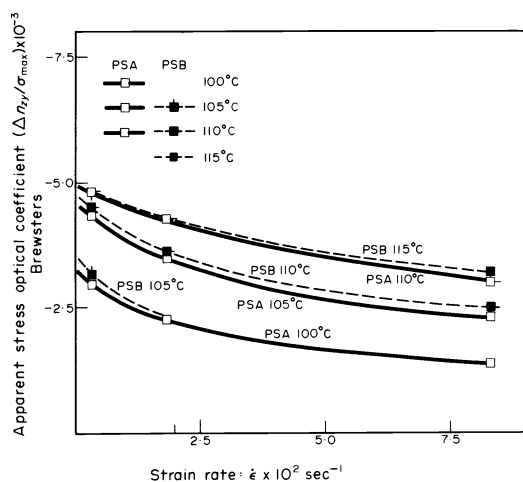


Fig. 7. Relationship between apparent stress optical coefficient and strain rate at different temperatures for PSA and PSB.

direction. This results in a negative birefringence with respect to the orientation direction.

In the glassy state the deformation is largely Hookean in character and the phenyl groups are compelled to be strained elastically in the direction of orientation. The birefringence is thus positive and the stress high for a small strain resulting in a very much reduced SOC in the region of about +10 Brewsters at room temperature and decreasing significantly as the temperature increases.<sup>16</sup> Thus in the region of the  $T_g$  this SOC is probably so small that it can be neglected in comparison with that due to the rubbery elastic deformation.

Rudd and Gurnee<sup>17</sup> recognised that these two kinds of deformation can occur simultaneously on stretching polystyrene in the vicinity of the  $T_g$  and that the stress of the Hookean elastic deformation relaxed very much more rapidly than that of the rubber or entropic elastic deformation. It is reasonable therefore to attribute the maximum shrinkage stress to entropic elastic deformation since the stress due to the Hookean elastic deformation would be essentially completely relaxed out during the heating up period of the determination. Hence as a first approximation the fraction of the total stress  $f = \sigma_{smax}/\sigma_{max}$  is that due to entropic elastic deformation and the remainder,  $(1-f)$ , that due to Hookean elastic deformation. Figure 8 shows how these stresses vary with strain rate, temperature and polymer molecular weight. Increasing temperature and decreasing strain rate favour entropic elastic deformation while decreasing temperature and increasing strain rate favour Hookean elastic deformation.

The entropic elastic deformation is due to the presence of time and temperature dependent chain entanglement. The higher the temperature and longer the time the easier it is for these entanglements to be resolved and for viscous flow to take place. Some measure of the degree of

entanglement is possible from a measure of the maximum shrinkage stress and the attendant length reversion ratio through the stress equation of rubber elasticity theory<sup>7,18</sup>

$$\sigma = NkT \left(1 - \frac{2Mc}{M}\right) \cdot \left(\frac{\bar{r}_i^2}{\bar{r}_0^2}\right) \cdot (\lambda^2 - \lambda^{-1})$$

$$= \frac{\rho RT}{Mc} \cdot \left(1 - \frac{2Mc}{M}\right) \cdot \left(\frac{\bar{r}_i^2}{\bar{r}_0^2}\right) \cdot (\lambda^2 - \lambda^{-1})$$

where  $\rho$  is the density of the melt,  $Mc$  the molecular weight between entanglements, and  $(\bar{r}_i^2/\bar{r}_0^2)$  is a term which measures the ratio of volume in the entangled state to that before and can be regarded as unity. From the experiments done with polymer A at two temperatures and at three strain rates the following values of  $N$  and  $Mc$  have been calculated taking the value of  $M$  the average molecular weight of the chains as 65,000 (Table 2).

A decrease in  $N$  and a corresponding increase in  $Mc$  is observed with increasing temperature while the effect of strain rate is just the reverse. The same pattern is true for PSB except that the effect of the molecular weight difference and the corresponding increase in  $T_g$  is to roughly double the value of  $N$  and halve the apparent value of  $Mc$  for the same conditions of temperature and strain rate.

It is also seen from Fig. 8 that increasing molecular weight apparently favours Hookean elastic deformation at the expense of entropic elastic deformation. However the comparison is made at a constant temperature of 110°C. It

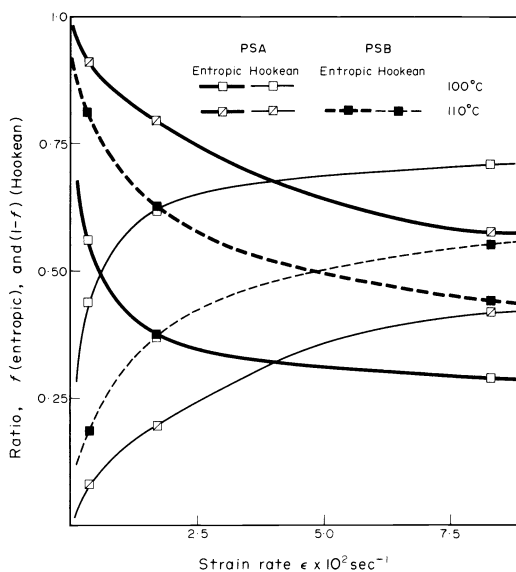


Fig. 8. Variation of ratio of Hookean and entropy elastic deformation stresses to total orientation stress with strain rate for PSA and PSB at two temperatures.

Table 2

Temperature		Strain rate		$\sigma_{smax}$		
°C	°K	(sec <sup>-1</sup> )	$\lambda = l_1/l_2$	(N . mm <sup>-2</sup> )	$N \times 10^{-19}$	$Mc$
100	373	$1.67 \times 10^{-2}$	3.588	3.061	6.67	$9.5 \times 10^3$
110	383	$0.33 \times 10^{-2}$	2.834	0.924	4.22	$1.50 \times 10^4$
110	383	$1.67 \times 10^{-2}$	3.449	1.419	4.26	$1.48 \times 10^4$
110	383	$8.33 \times 10^{-2}$	3.385	1.751	4.92	$1.29 \times 10^4$



is possible however by interpolation of the results of participant III L to compare the entropic elastic deformation for PSA and PSB at the same reduced temperature, i.e.  $T - T_g = \text{constant}$ . Participant IV took the values found by the differential scanning calorimeter of 93°C and 100°C for the  $T_g$  of PSA and PSB respectively and compared the values of the ratio  $f$  (entropic) at temperatures of 7°C and 12°C above these  $T_g$ 's for both polymers. The results are shown on Fig. 9.

It is now seen that PSB has a decidedly higher value for  $f$  (entropic) than PSA at both reduced temperatures and so increase in molecular weight now favours entropic elastic deformation.

From the value of the stress optical coefficient of polystyrene at a fixed temperature it is possible to obtain an estimate of  $(\alpha_1 - \alpha_2)$  the polarization anisotropy of the random molecular link from the equation

$$\text{SOC} = \frac{(\bar{n}^2 + 2)^2}{\bar{n}} \cdot \frac{2\pi}{45kT} (\alpha_1 - \alpha_2).$$

Taking a value of  $-5200$  Brewsters at 120°C the value of  $(\alpha_1 - \alpha_2)$  is  $-1.55 \times 10^{-23} \text{ cm}^3$ .

Gurnee<sup>19</sup> has calculated the polarization anisotropy of the styrene unit  $\alpha_z - \alpha_x$  when  $\alpha_z$  is the polarizability component along the polymer chain and  $\alpha_x$  at right angles to the chain i.e. along the axis of symmetry of the phenyl group. His value, using Denbigh's values of the principal polarizabilities of toluene,<sup>20</sup> and assuming restricted rotation of the phenyl group about its axis of symmetry of 45° is  $\alpha_z - \alpha_x = -5.5 \times 10^{-24} \text{ cm}^3$ . Although Gurnee<sup>19</sup> has neglected the contribution of the C-C and C-H bonds of the  $-\text{CH}_2-$  group in the chain, these bonds do contribute a polarization anisotropy of  $+0.6 \times 10^{-24} \text{ cm}^3$ . Saunders *et al.*<sup>21</sup> also find values varying from  $+0.9$  to  $+1.15 \times 10^{-24} \text{ cm}^3$  for the  $-\text{CH}_2-$  groups in various polyethylenes. In view of these results it is thought reasonable to take a value of say  $+1.0 \times 10^{-24} \text{ cm}^3$  as the contribution of the  $-\text{CH}_2-$  group to the polarization anisotropy of the styrene unit and thus  $\alpha_z - \alpha_x = -4.5 \times 10^{-24} \text{ cm}^3$ . Hence the number of monomeric units per random link is  $15.5/4.5$  say about 3.5. Hence, in spite of the bulk of the phenyl groups, the polystyrene chain would appear to be fairly flexible.

The influence of temperature and strain rate during orientation on the degree of entanglement of chains is also reflected in the degree of relaxation that takes place during the drawing as judged by the relationship between the draw ratio imposed and the length reversion ratio attained. Participant I studied this problem quite carefully by

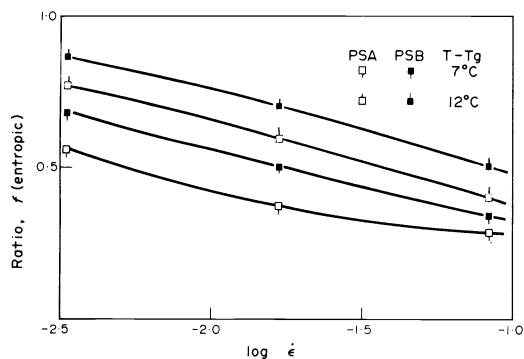


Fig. 9. Variation of ratio of entropy elastic deformation stress to total orientation stress with strain rate at constant reduced temperatures,  $T - T_g$  for PSA and PSB.

varying the temperature of draw from 100 to 120°C, the time of draw from 1 to 3000 sec and the draw ratio from 1.7:1 to 4:1.

Figure 10 summarises the results obtained at temperatures of 105° and 120°C and times of draw 1, 1500 and 3000 sec. These plots show the increasing relaxation that takes place on extending the time of draw or raising the temperature of draw. At 105°C little relaxation takes place even if the orientation takes place over 3000 sec while at 120°C some relaxation takes place within 1 second.

Accompanying the relaxation is a decrease in birefringence, but provided the temperature and time of draw are kept constant there is a linear relationship between the birefringence and the strain  $\epsilon$  as given by  $\epsilon = (DR - 1)$ . Since the birefringence is proportional to the stress required to orient the chains the ratio of the birefringence to the strain can be regarded as proportional to a time dependent relaxation modulus. The way in which this ratio varies with temperature at constant times of draw is shown on Fig. 11.

It can be seen from the way in which  $\Delta n_{xy}/\epsilon$  varies with temperature for constant times of draw that there is a rapid fall with temperature reminiscent of the fall in modulus with temperature at constant times or frequency. It can in fact be verified that the activation energy of the glass

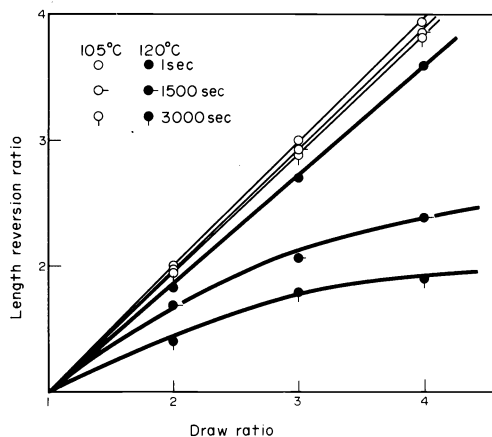


Fig. 10. Relationship between length reversion ratio and draw ratio at two temperatures and three times of draw for PSA.

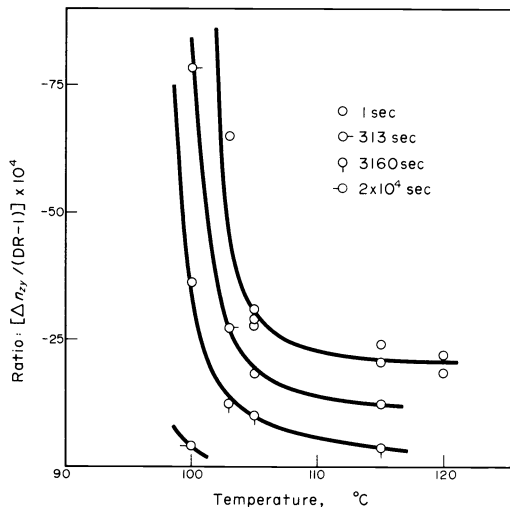


Fig. 11. Variation of the ratio  $\Delta n_{xy}/(DR - 1)$  with temperature at fixed times of draw for PSA.

transition of polystyrene also determines the time-temperature shift of the  $\Delta n_{xy}/\epsilon$  ratio. It is now evident that during the orientation of polystyrene at any temperature and time of draw the degree of orientation present in the final material is greatly dependent on the time taken and the temperature of orientation. It is seen however that the stress due to rubber-like elasticity which is latent in the glassy polymer is proportional to the birefringence and that both are direct measures of the extent of orientation.

#### 4.3.3 Birefringence and sonic modulus

The linear correlation expected between birefringence and orientation factor  $\alpha$  as given by the sonic modulus function  $(1 - E_u/E)$

$$\text{i.e. } \frac{\Delta n}{n_\alpha - n_\beta} = \alpha = (1 - E_u/E),$$

was investigated by participant I.

I measured the Young's modulus of specimens of the oriented PSA and PSB along the orientation direction by means of a flexural vibration apparatus at a frequency of about 200 Hz which corresponds to a time interval of about  $7.5 \times 10^{-4}$  sec, and by means of a high speed tensile test also operated in the time interval  $10^{-4}$ – $10^{-3}$  sec. The modulus remains essentially constant even beyond this time interval and may be considered as practically identical with the sonic modulus.

In Fig. 12 the values of  $(1 - E_u/E)$  are plotted against  $\Delta n$ . For both samples a linear relationship is obtained, as expected, but the slopes of the two lines are significantly different. It should be noted, however, that the observed changes in modulus are rather small: work on more extended polystyrene samples would be necessary before any definite conclusions can be drawn and the observed value of the slope compared with theoretical estimates of maximum birefringence ( $\alpha = 1$ ).

#### 4.4 Conclusions

In view of the good linear relationship found between birefringence and  $\sigma_{s,max}$  and the general agreement found between the estimate of SOC obtained from these quantities and those reported in the literature it may be taken that the oriented sheets supplied are extended rubbers which have been solidified in the extended state. Their birefringence can be taken as a direct measure of orientation but the degree is uncertain due to the ambiguity as to the birefringence of a fully extended chain. The

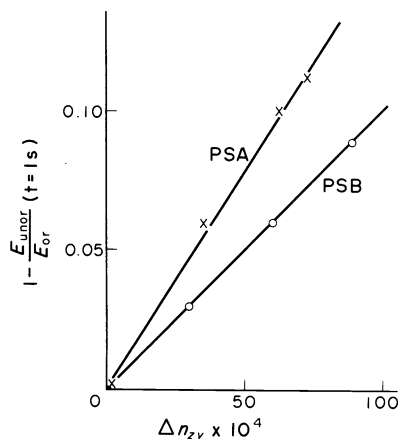


Fig. 12. Relationship between modulus and birefringence.

expected linear relationship between birefringence and the sonic modulus function  $(1 - E_u/E)$  is also observed but the relationship needs to be tested for material of much higher degrees of orientation than those studied here.

The nominal draw ratio and the length reversion ratio are not unequivocal estimates of the degree of orientation.

Birefringence will be used as a measure of degree of orientation in discussing the properties of the oriented materials in the remainder of this paper.

#### 5. SECTION (d) SOME PROPERTIES OF THE ORIENTED SHEETS

In the study of birefringence already discussed a knowledge of the tensile stress and strain in polymers when in the oriented rubbery state was required. The present section deals largely with tensile stress and strain relationships of the oriented polymers in the glassy state. Other aspects also considered will be impact behaviour and environmental stress cracking behaviour.

##### 5.1 Tensile properties

It is known that oriented structures become quite strong in the direction of orientation and correspondingly weak at right angles unless biaxial orientation is introduced. Nearly every participant therefore studied properties in tension at different strain rates and different angles to the orientation direction. The majority determined rupture stress while some paid attention to the yield stress and strain and to rupture strain. The energy required to rupture was also determined by some or could be estimated.

The tensile test piece agreed upon was that given in ISO Recommendation R527 Type 1 and most participants adhered to the dimensions specified but there were some small variations. The machining and finishing of the test pieces also differed slightly and ranged from the finish left by a high speed milling tool to polishing with a Silicon carbide paper, a benzene wetted pad or fusion.

All participants used an Instron Tensile Tester except VII who used an adapted Schopper apparatus with tensometric loading device. In addition I used a Plastechon Mod. 581 High Speed Tester and IV a modified impact pendulum capable of recording load-time plots,<sup>22</sup> for high speed testing.

5.1.1 *The estimation of strain rate.* In order to compare the results of the participants on a common basis it was necessary to select independent parameters which each participant had used or which could be estimated from the results submitted. The birefringence used as a measure of degree of orientation of course is one such parameter. Another parameter selected was the strain rate. If an estimate of the strain rate can be carried out for all the participants, at least as far as the yield point, then this can form a basis for comparing results. An estimate of the strain rate can be arrived at from a knowledge of the dimensions of the actual test piece used, the cross-head speed, and the initial distance apart of the grips. The method of calculation is given in the Appendix.

Participant I also made a careful note of the time required to yield and to rupture. These times can also be calculated from the yield strain and rupture strain and the strain rate, and can be used as the independent parameters for comparing properties.

5.1.2 *The estimate of specific rupture energy,  $W_r$ .* Not all participants measured the specific rupture energy,  $W_r$ , which defines the energy expended to rupture per unit volume.

Participant I measured the area under the stress/elongation plot which gives the energy required to break unit area of that particular specimen. If this quantity is divided by the length of the necked narrow portion into which the energy required to extend the remainder of the sample is largely released at rupture a good estimate of the rupture energy per unit volume is obtained.

Participant II noted the stress and elongation at yield and stress and elongation at rupture. This information, the cross head speed and the dimensions of the sample enable the strain of the narrow portion at yield and at rupture to be calculated. From the stress-strain relationship thus available the rupture energy per unit volume can be estimated.

**5.1.3 The variation of rupture stress with strain rate and orientation.** All the participants measured rupture stress,  $\sigma_r$ , at various strain rates and with test pieces cut at  $0^\circ$ ,  $45^\circ$  and  $90^\circ$  to the orientation direction. Figure 13 shows how  $\sigma_r$  varies with birefringence for different strain rates at each of the three angles for PSA.\*

For the  $0^\circ$  samples increasing strain rate and birefringence in general improve  $\sigma_r$ . For the lowest strain rates however increasing orientation does not necessarily cause improved strength and this is associated with yielding before rupture. The  $45^\circ$  samples also improve in rupture stress with orientation and strain rate but not as rapidly as the  $0^\circ$  samples. However, due to the yielding before rupture that takes place with  $0^\circ$  samples with increasing birefringence at low strain rates the  $45^\circ$  samples are seen to be actually stronger under these conditions since they break without yielding.

The  $90^\circ$  samples show a consistent fall in strength with orientation while strain rate again improved strength in general.

The lower strength values found by participant VII are believed due to the finishing of the edges of the test samples by fusion.

\*In Figs. 13-15 inclusive experimental points have small figures alongside. These denote the estimated strain rates as follows: 5 represents  $10^{-5} \text{ sec}^{-1}$ ; 4 represents  $10^{-4} \text{ sec}^{-1}$ ; 3 represents  $10^{-3} \text{ sec}^{-1}$ ; 1 represents  $6.1 \times 10^{-2} \text{ sec}^{-1}$ ; 50 represents  $50 \text{ sec}^{-1}$ ; 260 represents  $260 \text{ sec}^{-1}$ . The letter Y denotes yielding.

There was not a great deal of difference between PSA and PSB except that the latter was slightly stronger.

Some tests done by participant III on PSB in bending gave rise to significantly higher rupture stresses of almost 3 times those in tension for the same strain rate. This is believed to be due to the fact that the surface under greatest stress in a flexure test is the virgin surface of the oriented sheet which has not been machined.

**5.1.4 The variation of rupture strain with strain rate and orientation.** Participants I, II, IV and VI measured rupture strain  $\epsilon_r$  directly or the elongation at break  $\Delta l$ , from which it could be calculated. The results are plotted on Fig. 14 against birefringence for different strain rates and at each of the three angles for PSA.

At  $0^\circ$  improvement in rupture strain is observed with increasing birefringence particularly at low strain rates where very large increases in rupture strains occur for both polymers. PSB in particular reaches very high values as much as 46% for the highest birefringence and lowest strain rate. These high rupture strains are indeed the result of yielding without crazing. As strain rate is increased the rupture strains at  $0^\circ$  decrease particularly at high orientations the lowest strains being recorded at  $50 \text{ sec}^{-1}$ . The apparent increase at  $260 \text{ sec}^{-1}$  is believed due to the use by Participant IV of smaller ASTM D 1822 Type S specimens which may be less subject to flaws. An apparent maximum in rupture strain is indicated at about  $10^{-1} \text{ sec}^{-1}$  at low birefringence.

At  $45^\circ$  effects are not as marked as for  $0^\circ$  samples but the general pattern of improvement of  $S_r$  with birefringence is true at low birefringences but maxima in  $\epsilon_r$  are observed as birefringence increases. In general increase in strain rate decreases  $\epsilon_r$  except at low birefringencies when there again appears to be a maximum at about  $10^{-1} \text{ sec}^{-1}$ .

At  $90^\circ$  the  $\epsilon_r$  is quite small at high birefringences and has been plotted on a logarithmic scale to prevent confusion. Increasing birefringence causes a decrease in  $\epsilon_r$  at all strain rates. The effect of strain rate would appear to be an improvement in  $\epsilon_r$ , as far as  $10^{-1} \text{ sec}^{-1}$  then a decrease at  $50 \text{ sec}^{-1}$ . The anomalous high position of the  $260 \text{ sec}^{-1}$  plot is again believed associated with shorter test specimens.

**5.1.5 The variation of specific rupture energy,  $W_r$ , with strain rate and orientation.** The specific rupture energy,  $W_r$ , of course combines the stress and the strain behaviour

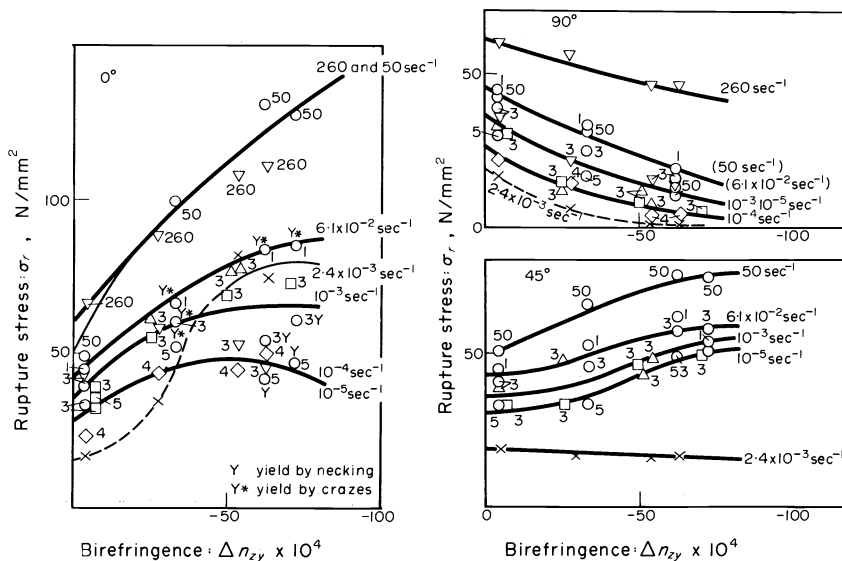


Fig. 13. Variation of rupture stress,  $G_r$ , with birefringence for different strain rates at angles  $0^\circ$ ,  $45^\circ$  and  $90^\circ$  to the draw direction for PSA.

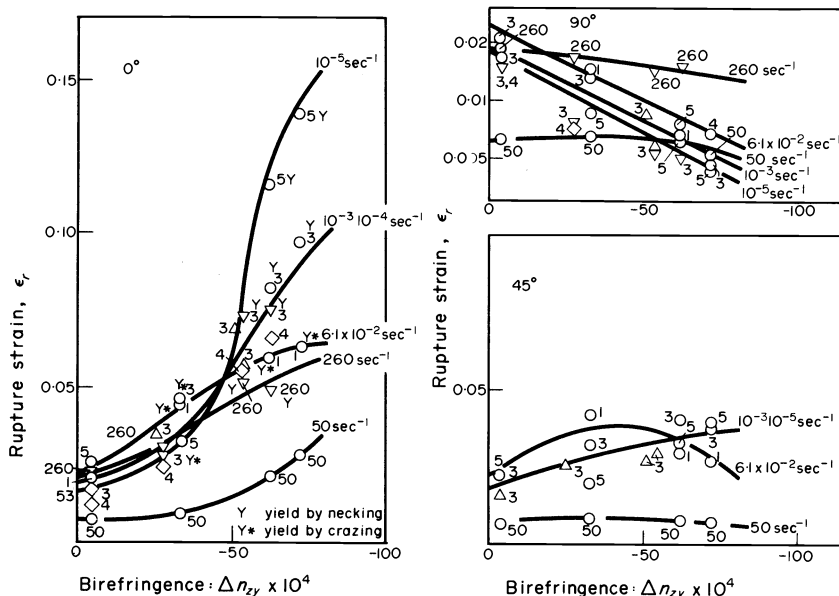


Fig. 14. Variation of rupture strain,  $\epsilon_r$ , with birefringence for different strain rates at angles  $0^\circ$ ,  $45^\circ$  and  $90^\circ$  to the draw direction for PSA.

to the point of rupture and Fig. 15 shows how  $W_r$  varies with birefringence at the difference strain rates for each of the three angles for PSA.

At  $0^\circ$  increasing birefringence improves the rupture energy but it does not increase as much as the rupture strain under yielding conditions due to the decrease in rupture stress that ensues. Apart from the maximum at a strain rate of about  $10^{-1} \text{ sec}^{-1}$  at low birefringences, increasing strain rate generally causes a decrease in  $W_r$  with the experiments at  $260 \text{ sec}^{-1}$  again giving increased values.

For  $45^\circ$  samples increased birefringence does not produce a marked improvement and the results at about  $10^{-1} \text{ sec}^{-1}$  do in fact exhibit a maximum. This also results in

a maximum with increasing strain rate at low birefringences and a decrease in  $W_r$  with strain rate at higher birefringences. For  $90^\circ$  samples which have been plotted on a logarithmic scale since they become so small the effect of increasing birefringence is a decided reduction in  $W_r$ . However there appears to be an improvement in  $W_r$  with strain rate but the results at  $50 \text{ sec}^{-1}$  tend to be somewhat out of line. The results at  $260 \text{ sec}^{-1}$  again are distinctly higher than the other strain rates particularly at high birefringences.

PSB behaves in a similar manner to PSA except that the values of  $W_r$  are in general greater.

5.1.6 Variation of rupture strain with time to rupture. Another way of examining the stress/strain relationships is

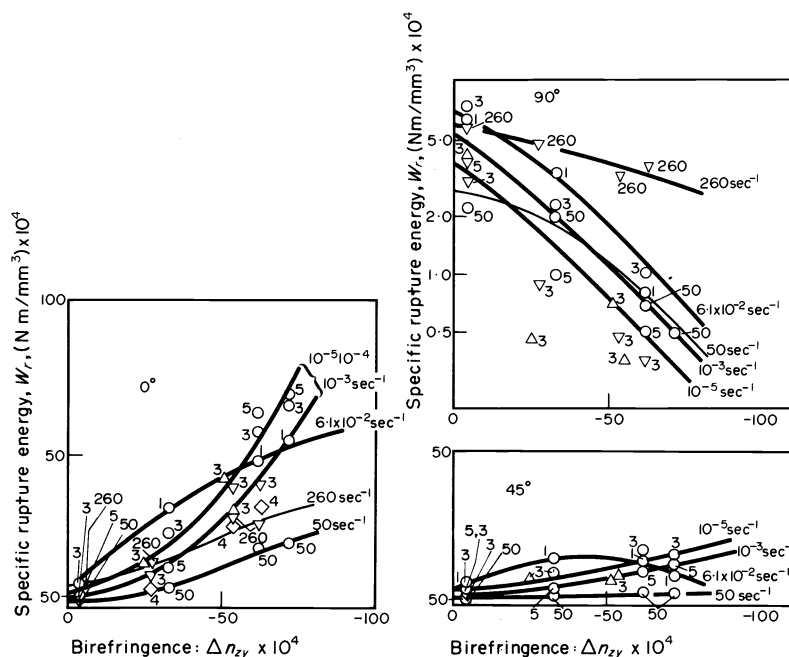


Fig. 15. Variation of specific rupture energy,  $W_r$ , with birefringence for different strain rates at angles  $0^\circ$ ,  $45^\circ$  and  $90^\circ$  to the draw direction for PSA.

in terms of the time required to produce the effect rather than in terms of strain rate. It has already been commented on how variation of strain rate has produced certain effects e.g. maxima in  $\epsilon_r$  at low birefringences. Since the time to yield or rupture is in general inversely related to strain rate it might be expected that such maxima should be observed as time to yield or time to rupture varies. Participant I in particular measured yield time and rupture time while the time to rupture could be calculated from the results of II, IV and VI. Oberst and Retting<sup>4</sup> have shown that behaviour in the non-linear region such as rupture strain,  $\epsilon_r$ , is influenced by molecular relaxation processes in the range of small deformations and the effect of these relaxation processes may be seen by observing the time to rupture,  $t_r$ , as an independent parameter. Figure 16 illustrates the way in which  $\epsilon_r$  varies with  $t_r$  for each NDR, at 0° and 90° to the direction of orientation for PSA. For the nominally unoriented polymer there is evidence of a maximum in the region of about 1 sec for  $t_r$ . This maximum moves to longer times with orientation and becomes amplified for 0° samples while the reverse is true for 90° samples. It is believed that this transition is due to the secondary or  $\beta$  relaxation process of polystyrene which occurs at about 20°C at 1 Hz ( $t = 0.16 \text{ sec}^{23-25}$ ). Orientation therefore causes a shift in the relaxation process to longer times at constant temperatures or higher temperatures at constant times. This would suggest that it is becoming more difficult for the motion to take place in the orientation direction. This is not unreasonable in the oriented state where the entropy is less. In addition, for 90° samples the reverse appears to be true, i.e. the more restricted the chain motion becomes in the orientation direction the easier it is to separate the chains at right angles. The effect in fact is more marked for PSB than PSA. Further light on the above proposal is obtained from a study of the time dependent Young's Modulus of Elasticity which is discussed in the next paragraph.

5.1.7 *The time dependent Young's Modulus of Elasticity,  $E(t)$  and the relaxation spectrum  $H(\ln \tau)$ .* Participant I carried out a detailed study of the time dependent Young's

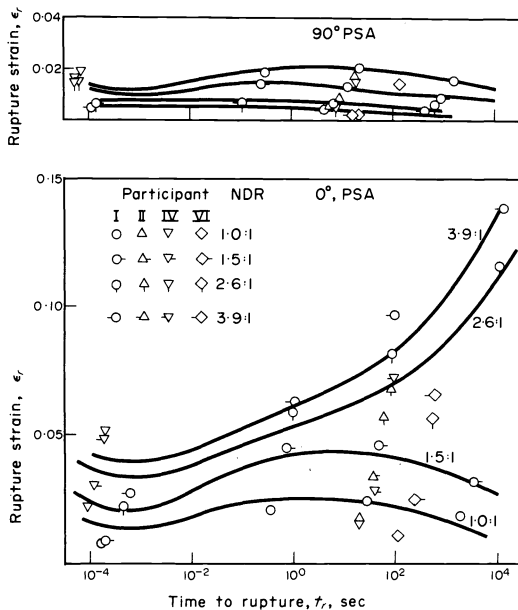


Fig. 16. Relationship between rupture strain,  $\epsilon_r$ , and time to rupture,  $t_r$ , for each nominal draw ratio and at angles of 0° and 90° to the direction of orientation for PSA.

Modulus  $E(t)$  following the principles described in the paper by Oberst and Retting<sup>4</sup> on a similar study on PVC which originated within the present Working Party. The time dependent modulus  $E(t)$  is the stress relaxation modulus at appointed times,  $t$ , and can yield through the relationship:

$$E(t) = \int_{-\infty}^{+\infty} H(\ln \tau) e^{-t/\tau} d(\ln \tau),$$

a measure of the relaxation spectrum  $H(\ln \tau)$ . For long times the value of  $E(t)$  may be obtained in the usual way from stress relaxation experiments. For shorter times, tensile tests at constant strain rates yield  $E(t)$  through the tangential modulus  $d\sigma/d\epsilon$  measured at the appointed time,

$$\text{i.e. } d\sigma/d\epsilon = E(t).$$

For very short times the storage modulus  $E'$  in flexural vibration experiments carried out at different frequencies,  $\omega$ , is a measure of  $E(t)$  where time is defined at  $t = 1/\omega$  i.e.  $E'(\omega) \approx E'(t)_{t=1/\omega}$ . The results of these studies over a time range of  $10^{-4}$ – $10^4$  sec are given on Fig. 17 for PSA and PSB for the various draw ratios and for angles of 0° and 90° to the draw direction.

The increase in  $E(t)$  with orientation at short times has already been mentioned in connection with the relationship between birefringence and sonic modulus at 0° to the direction of orientation. This increase is clearly seen in the above figures and it persists with increasing time. At 90° the modulus falls with orientation although not much information was available for PSA.

There is little to choose between PSA and PSB at very short times, but as time increases both polymers exhibit a decrease in modulus for all draw ratios and both angles. For PSB this decrease does not start to be significant until times of 1 sec and over are reached. For PSA however the decrease starts much sooner, probably at a time of  $10^{-4}$  sec, which agrees with its lower  $T_g$ .

In order to obtain the relaxation spectrum  $H(\ln \tau)$  a first order approximation is given by the expression<sup>4,26</sup>

$$H(\ln \tau) \approx - \left. \frac{dE(t)}{d(\ln t)} \right|_{t=\tau} = - E(t) \left. \frac{d(\log E(t))}{d(\log t)} \right|_{t=\tau}.$$

Hence if  $\log E(t)$  is plotted against  $\log t$  and the slope at specified times  $t$  is multiplied by the value of  $-E(t)$  at that time then the product to a first approximation is the value of  $H(\ln \tau)$  at that time.

Figure 18 shows the relaxation spectra obtained in this way for PSA for the draw ratio 1.0:1 and 3.9:1. A decided shift of the spectrum towards longer times is seen on increasing the draw ratio in support of the shift of the  $\epsilon_r$  vs  $t_r$  maximum towards longer times shown on Fig. 16. The spectra are in the appropriate position to correspond with the  $\beta$  relaxation of polystyrene and if experiments had been conducted over a similar range of times at higher temperatures it would be expected that the  $\beta$  relaxation spectrum would move to shorter times.

5.1.8 *The effect of temperature on tensile properties.* Although the effect of temperature on the time dependent modulus  $E(t)$  over a wide time spectrum was not carried out, Participant VI did study the tensile properties of PSA and PSB at 40°C and 60°C as well as at 23°C at one strain rate namely  $1.1 \times 10^{-4} \text{ sec}^{-1}$ . The results of this work are shown on Fig. 19 where rupture properties are plotted against birefringence for the three temperatures and for angles of 0° and 90°.

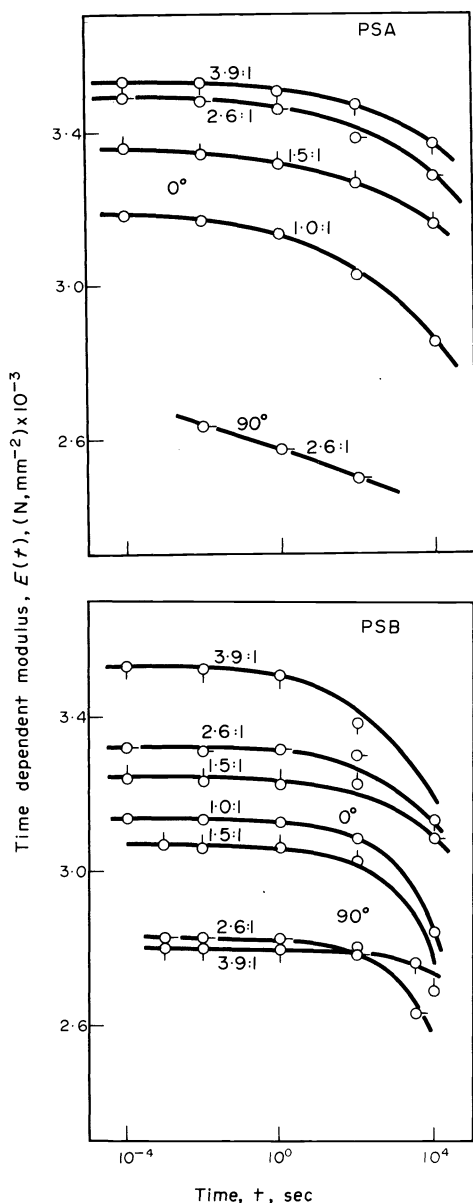


Fig. 17. Relation between the time dependent modulus,  $E(t)$ , and the time,  $t$ , for PSA and PSB at the various nominal draw ratios and at angles of  $0^\circ$  and  $90^\circ$ .

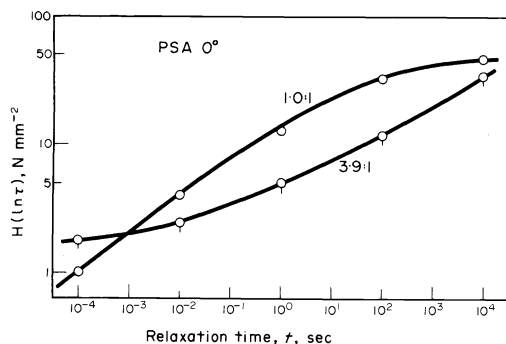


Fig. 18. Relaxation spectra for PSA at NDR = 1.0:1 and 3.9:1 and at angle  $0^\circ$ .

As temperature is increased  $\sigma_r$  at an angle of  $0^\circ$  decreases while  $\epsilon_r$  increases particularly at high birefringence due to yielding. The nett result of these two effects is a decrease in  $W_r$  with temperature at low birefringence and then an increase to quite high values at higher birefringences. Specimens cut at  $90^\circ$  become very weak as temperature and birefringence increase and although temperature does improve  $\epsilon_r$  slightly the nett effect on  $W_r$  is to reduce it to quite small values.

The behaviour of PSB was similar to that of PSA except that the effects of temperature on  $\epsilon_r$  and  $W_r$  were more marked while  $\sigma_r$  was not greatly different. Participant VI also studied the effect of temperature on the storage modulus  $E'$  at 200 Hz which corresponds to a time of about  $8 \times 10^{-4}$  sec. The results of this work are shown on Fig. 20 for PSA and PSB for undrawn and 3.9:1 NDR material. This shows the effect of temperature in reducing  $E'$  as well as the effect of orientation in increasing the modulus for  $0^\circ$  samples and decreasing it for  $90^\circ$  samples. The effect of increasing temperature in decreasing the modulus is similar to that of increasing time as shown on Fig. 17.

### 5.2 Impact strength

A study of impact strength was carried out by Participants I, II, IV, VI and VII using essentially similar methods based on the Charpy flexural impact test, using unnotched specimens,  $50 \text{ mm} \times 6 \text{ mm} \times 3 \text{ mm}$ , placed against two anvils 40 mm apart and broken by a hammer travelling at  $290 \text{ cm sec}^{-1}$  which corresponds to a strain rate of approximately  $32.6 \text{ sec}^{-1}$  for the portion that ruptures first opposite the point of impact.

IV also used a span of 100 mm and a hammer speed of  $345 \text{ cm. sec}^{-1}$  which results in a reduced strain rate of  $6.2 \text{ sec}^{-1}$ .

The results of these experiments are shown on Fig. 21 on a logarithmic scale against birefringence. As orientation increases very high impact strengths are observed for specimens cut at  $0^\circ$  to the direction of orientation and correspondingly very low values for those cut at  $90^\circ$ . For the  $45^\circ$  samples a flat maximum is observed reminiscent of the behaviour in tension. PSB is seen to be stronger than PSA but not unduly so. When the conditions of test are varied as done by IV by increasing the span which causes a fall in strain rate as well as increasing the volume of material under stress, the impact strength is seen to increase as shown by the dotted lines.

Participants VI and VII also notched their samples with 1 mm deep and 0.8 mm wide notches. The well known reduction in impact strength was observed as shown on Fig. 22. The notch has the effect of confining the volume under greatest strain to that portion beneath the root of the notch and so the work of rupture is also confined to this volume which is a good deal smaller than the volume involved in rupture when unnotched. In addition, the effective span of the test piece is a good deal shorter because of the notch and so the strain rate is correspondingly greater. This may also cause a reduction in impact strength.

While the notched impact strength is lower than for the unnotched, the effect of orientation is to increase the value for  $0^\circ$  samples, there is also a continuing increase for the  $45^\circ$  samples and the  $90^\circ$  samples do not decrease as rapidly as for unnotched samples.

### 5.3 Environmental stress cracking

Another important aspect of the strength properties of polymers is their resistance to cracking when immersed in

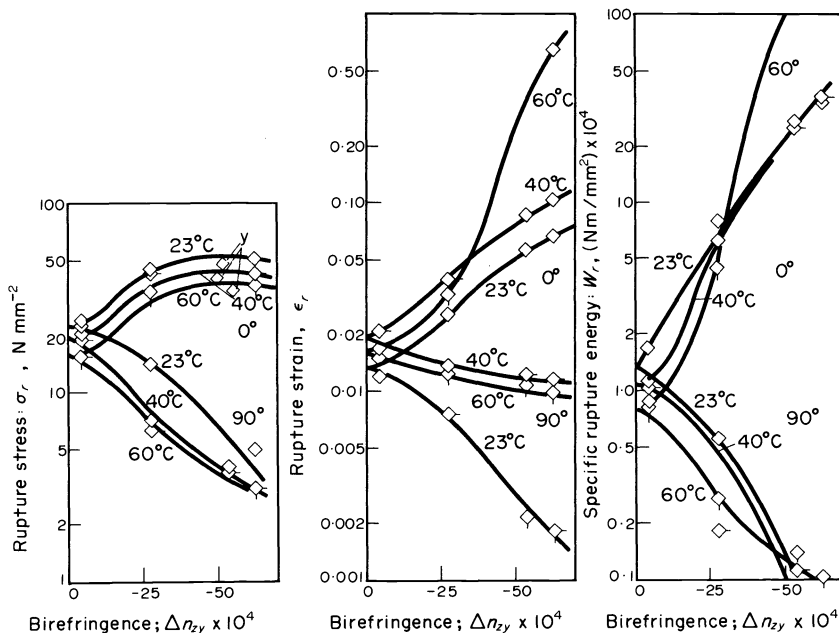


Fig. 19. Effect of temperature and birefringence on rupture stress,  $\sigma_r$ , rupture strain,  $\epsilon_r$ , and specific rupture energy,  $W_r$ , for PSA at angles 0° and 90° and constant strain rate,  $1.1 \times 10^{-4} \text{ sec}^{-1}$ . (Participant VI.)

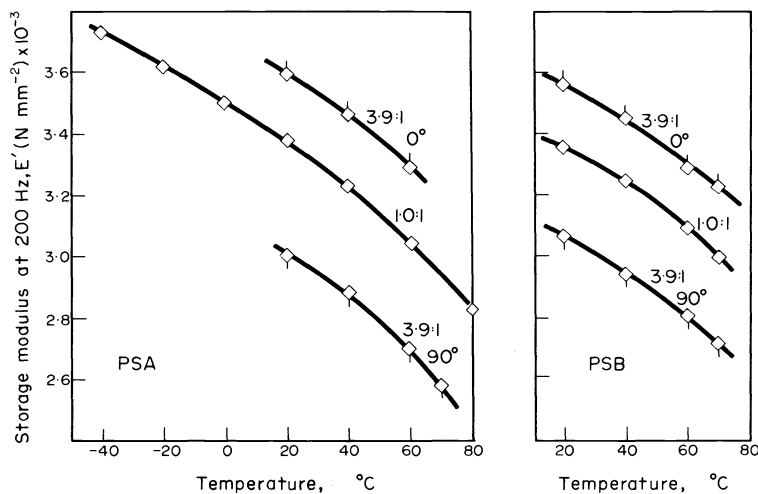


Fig. 20. Effect of temperature on storage modulus,  $E'$  (200 Hz) of PSA and PSB for 1.0:1 and 3.9:1 NDR samples and angles 0° and 90°.

certain media which can diffuse into the structure and give rise to internal stresses.

Participant I examined the behaviour of the oriented polystyrenes immersed in one such media namely a mixture of 1:5 volumes of *n*-heptane/*iso*-propyl alcohol at 23° for 60 min. Circular holes 3 mm in diameter are drilled through the oriented sheet specimens and steel balls of slightly oversize diameter are pressed into the holes, the oversize increasing regularly so as to give rise to increasing strains. The mixture causes cracks to grow around the holes the length and direction of which depend on the oversize of the ball and the orientation of the specimen.

The results are given on Fig. 23 as plots of the length of the cracks along the orientation direction against the uniaxial strain caused by the oversize of the ball for each polymer and each draw ratio.

It is seen that crack length is both a function of the strain imposed and the degree of orientation and that PSA is a

good deal less resistant than PSB. It appears that at the higher draw ratios, and moreso for PSA than PSB, an upper strain limit exists the exceeding of which causes a catastrophic crack growth.

## 6. SUMMARY AND CONCLUSIONS

This paper seeks to consider some of the consequences of orienting a typical non-crystalline atactic homopolymer namely polystyrene. Two commercial polystyrenes of different molecular weight, glass transition temperatures and rheological properties were chosen for study and the properties studied included the length reversion ratio, the birefringence, the orientation stress, the shrinkage stress and various mechanical properties such as the rupture stress and strain, the specific energy of rupture, the sonic modulus, the relaxation modulus, impact behaviour and environmental stress cracking behaviour. The two polymers were sheet extruded and then drawn to the same

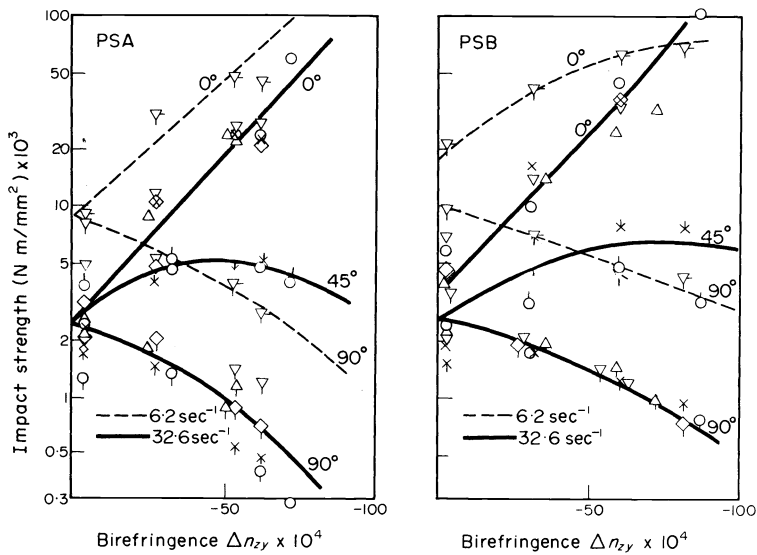


Fig. 21. Impact strengths of PSA and PSB plotted against birefringence for various angles to the orientation direction and at two strain rates. Un-notched samples.

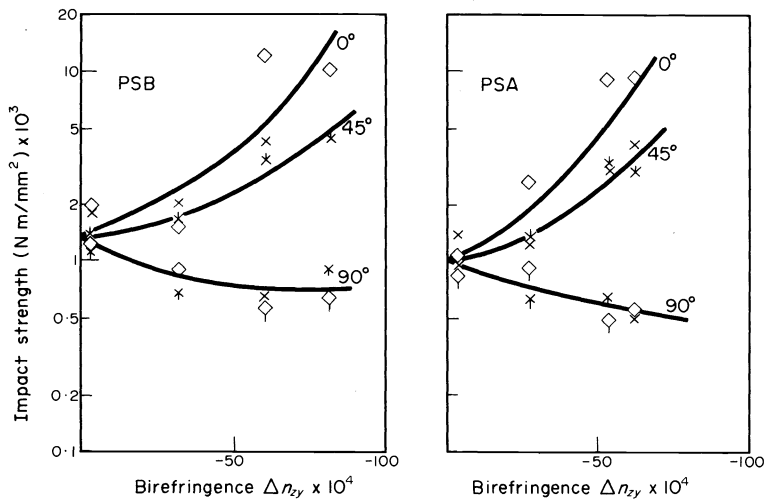


Fig. 22. Impact strengths of notched samples of PSA and PSB plotted against birefringence for various angles to the orientation direction at a strain rate of 32.6 sec<sup>-1</sup>.

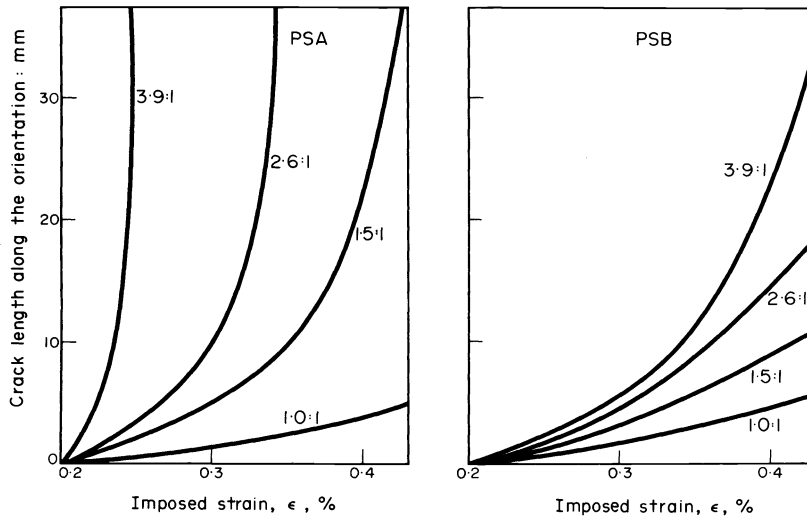


Fig. 23. Relationship between crack length along the orientation direction and the imposed strain.



nominal draw ratios, but the length reversion ratios that resulted were always a little higher than the NDR due to some orientation being imparted before the orientation step except at the highest NDR where some relaxation took place during the drawing operation owing to the higher temperatures required. There was good agreement between the LRR for polystyrene A and polystyrene B for any NDR.

When birefringence is compared with NDR it does not increase as quickly as NDR while PSB has a higher value than PSA. This latter feature is accentuated when birefringence is plotted against LRR i.e. for any value of LRR the birefringence of PSB is greater than that of PSA. This is reasonable since the viscosity of PSB at any one temperature is higher than that of PSA. However, the birefringence does not increase rapidly enough to satisfy rubber elasticity theory and this is attributed to the fact that the sheets were subjected to different strain rates and temperatures during orientation which would influence the degree of temporary chain entanglement, hence the orientation stress and so the birefringence.

Birefringence is shown to be a quantitative measure of orientation of PSA and PSB and the linear relationship between it and the stress required to orient the polystyrene at temperatures in the vicinity of  $T_g$  is in two parts, one produces Hookean elastic extension while the other results in rubber-like or entropic extension. The Hookean elastic extension is small in magnitude but high in stress which relaxes very quickly and is associated with a small positive stress optical coefficient. The rubber-like extension on the other hand is large in magnitude for the same order of stress which requires much longer to relax and is associated with a large negative SOC.

The relative amounts of the two stress components during any orientation procedure are greatly dependent on the strain rate and the temperature, increasing temperature and low strain rates favouring rubber-like extension. The degree of entanglement present during rubber-like extension is also dependent on temperature and strain rate, the higher the temperature and lower the strain rate the smaller is the degree of entanglement. The temperature and strain rate also influence the degree of relaxation as judged by the relationship between the draw ratio imposed and the LRR attained, increasing temperature and times of draw favouring relaxation and a decrease in LRR. The same effect is found for the birefringence of the resulting oriented material which can be shown to decrease quite rapidly with increasing temperatures and times of draw for the same NDR. Tensile rupture properties of the oriented polymers in the glassy state i.e. rupture stress, rupture strain and specific rupture energy are shown to be dependent on the degree of orientation, the strain rate and the angle of the long axis of the specimen to the orientation direction. There is also evidence that the dimensions of the sample and the finish can influence the properties.

In general for  $0^\circ$  samples increasing orientation improves rupture stress, rupture strain and specific rupture energy. At high orientations however due to the onset of yield by necking a decrease in rupture stress occurs at low strain rates. Another effect also is that at low orientations there is an apparent maximum in rupture strain as strain rate is increased but at higher orientations strain rate causes a decrease in rupture strain. The use of a shorter test piece at an even higher strain rate reverses this trend and this is attributed to a shorter sample having less flaws. For  $45^\circ$  samples the properties do not change markedly with orientation except to improve slightly for rupture stress

since no yielding is present for these samples and an apparent maximum in rupture strain at low orientations as strain rate is increased.

For  $90^\circ$  samples there is a decided fall in all properties with birefringence with rupture stress, rupture strain and specific rupture energy improving with strain rate.

If time to rupture is taken as an independent parameter for the study of rupture strain then a maximum in rupture strain is observed with increasing time for the unoriented material at  $0^\circ$ . This maximum appears also in the 1.5:1 NDR material but amplified and at a longer time and it would seem it would appear at still longer times further amplified at higher orientation. This maximum is believed to be due to the  $\beta$  relaxation process of polystyrene and the maximum observed in  $\epsilon_r$  with strain rate is also attributed to the same process. For  $90^\circ$  samples the above effects are reversed.

The movement of the relaxation process to longer times with orientation at  $0^\circ$  is in keeping with the process becoming more difficult with orientation and conversely at  $90^\circ$ . The effect is more marked for PSB than for PSA. Some evidence for the existence of the  $\beta$  process is also seen from the relaxation spectrum obtained from plots of the time dependent modulus  $E(t)$  against log time. It is believed that the short time flank of the  $\beta$  process is seen for the unoriented material and that this shifts to longer times for the 3.9:1 NDR material.

The effect of increase in temperature at one low strain rate has resulted in a decrease in  $\sigma_r$  at  $0^\circ$  and an increase in  $\epsilon_r$ , particularly at high orientations due to yielding. The net effect on  $W_r$  is to decrease it as temperature increases at low birefringences and then to increase it at high birefringences.

At  $90^\circ$  the general effect of increase in temperature is to depress all rupture properties.

The effect of temperature on the storage modulus  $E'$  at 200 Hz is a uniform decrease in value similar to the decrease in time dependent modulus  $E(t)$  with increasing time at constant temperature. The oriented materials at  $0^\circ$  and  $90^\circ$  also exhibit the same decrease in  $E'$  with temperature.

Charpy impact testing at one hammer speed show the very high impact strength resulting from orientation for  $0^\circ$  samples and the correspondingly very low values for  $90^\circ$  samples with PSB slightly stronger than PSA.

A decrease in hammer speed and increase in span improve impact strength due probably to decrease in strain rate and the larger volume involved in the rupture process. The effect of notching is to reduce the impact strength due presumably to the reverse effects.

The environmental stress cracking experiments showed that the oriented polymers subjected to lateral strains can develop catastrophic crack growth when immersed in an active liquid. The onset of the cracks depends on the lateral strain imposed, and the degree of orientation. PSB was found to be more resistant than PSA.

#### REFERENCES

- <sup>1</sup>T. T. Jones, *J. Polymer Sci.* **16C**, 3845 (1968).
- <sup>2</sup>A. Gonze, *Pure Appl. Chem.* **18**, 553 (1969).
- <sup>3</sup>J. L. S. Wales, *Pure Appl. Chem.* (1968); and **20**, 331 (1969).
- <sup>4</sup>H. Oberst and W. Retting, *J. Macromol. Sci. Phys.* **B5(3)**, 559 (1971).
- <sup>5</sup>A. Gonze and J. Chauffoureaux, *Pure Appl. Chem.* **35**, 315 (1973).
- <sup>6</sup>A. J. de Vries and M. Carrega, IUPAC Working Party Report, September (1971).
- <sup>7</sup>L. R. G. Treloar, *The Physics of Rubber Elasticity*. Clarendon Press, Oxford (1949).

<sup>8</sup>P. H. Hermans, *Physics and Chemistry of Cellulose Fibres*. Chap. 5. Elsevier, New York (1949).  
<sup>9</sup>W. W. Moseley, Jr., *J. Appl. Polym. Sci.* **3**, 266 (1960).  
<sup>10</sup>H. W. Morgan, *Textile Res. J.* **32**, 866 (1962).  
<sup>11</sup>H. De Vries, *On the Elastic and Optical Properties of Cellulose Fibres*. Utrecht, Schotanus Jens (1953).  
<sup>12</sup>J. L. S. Wales and H. Janeschitz-Kriegl, *Rheol. Acta* **7**, 19 (1968).  
<sup>13</sup>L. E. Nielsen and R. Buchdahl, *J. Colloid Sci.* **5**, 282 (1950).  
<sup>14</sup>J. F. Rudd and R. O. Andrews, *J. Appl. Phys.* **29**, 1421 (1958).  
<sup>15</sup>G. L. Wilkes and R. S. Stein, *J. Polym. Sci. A-2*, **7**, 1525 (1969).  
<sup>16</sup>J. F. Rudd and E. F. Gurnee, *J. Appl. Phys.* **28**, 1096 (1957).  
<sup>17</sup>J. F. Rudd and E. F. Gurnee, *J. Polym. Sci. A.1*, 2857 (1963).  
<sup>18</sup>P. Meares, *Polymers: Structure and Bulk Properties*. Van Nostrand, New York (1965).  
<sup>19</sup>E. F. Gurnee, *J. Appl. Phys.* **25**, 1232 (1954).  
<sup>20</sup>K. G. Denbigh, *Trans Faraday Soc.* **36**, 936 (1940).  
<sup>21</sup>D. W. Saunders, D. R. Lightfoot and D. A. Parsons, *J. Polym. Sci. A-2*, **6**, 1183 (1968).  
<sup>22</sup>T. Casiraghi, *Materie Plastiche* **36**, 1053 (1970).  
<sup>23</sup>J. Heijboer, *Physics of Non-Crystalline Solids*. Delft (1964).  
<sup>24</sup>N. G. McCrum, B. E. Read and G. Williams, *Anelastic and Dielectric Effects in Polymer Solids*. Wiley, New York (1967).  
<sup>25</sup>O. Yano, and Y. Wada, *J. Poly. Sci. A-2*, **9**, 669 (1971).  
<sup>26</sup>A. J. Staverman and F. Schwarzl, *Die Physik der Hochpolymeren* (editor H. A. Stuart) Vol. 4, Chap. 1. Springer, Berlin (1956).

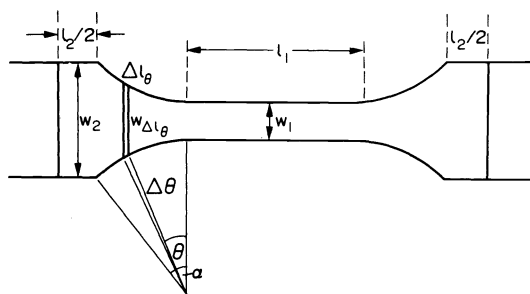


Fig. A1.

strain rate of a small element of length  $\Delta l_\theta$  situated at an angle  $\theta$  from the radius normal to one end of the inner narrow portion and  $\dot{\epsilon}_2$  is the strain rate of the outer wider portion.

It can also be shown that provided all parts of the structure are obeying Hooke's Law then

$$\dot{\epsilon}_1 w_1 = \dot{\epsilon}_{\Delta l_\theta} w_{\Delta l_\theta} = \dot{\epsilon}_2 w_2 \tag{A.2}$$

where  $w_{\Delta l_\theta}$  is the width of the small element of length  $\Delta l_\theta$ .

The value of

$$w_{\Delta l_\theta} = W_1 + 2r(1 - \cos \theta) \tag{A.3}$$

the full magnitude of  $\theta$  namely  $\alpha$  being determined by the value of  $r$ ,  $w_1$  and  $w_2$  in that

$$\cos \alpha = \frac{r - (w_2 - w_1)/2}{r} \tag{A.4}$$

Substituting for  $\epsilon_{\Delta l_\theta}$  and  $\epsilon_1$  in equation (A.1) from equation (A.2) it follows that

$$K = l_1 \dot{\epsilon}_1 + 2r w_1 \dot{\epsilon}_1 \int_0^\alpha \frac{\cos \theta d\theta}{w_1 + 2r(1 - \cos \theta)} + \frac{l_2 \dot{\epsilon}_1 w_1}{w_2}$$

From which  $\dot{\epsilon}_1$  may be calculated.

APPENDIX

Estimate of strain rate in stress/strain experiments in tension

If the test piece is divided into three portions namely the narrow inner part of length  $l_1$  and width  $w_1$ , the curved portion of radius  $r$  and the outer wider portion which is gripped, the distance between the grips and the outer limit of the curved portion being  $l_2/2$  and the width  $w_2$  then it can be shown that if  $K$  is the constant crosshead speed

$$K = l_1 \dot{\epsilon}_1 + 2 \int_0^\alpha \Delta l_\theta \dot{\epsilon}_{\Delta l_\theta} + l_2 \dot{\epsilon}_2 \tag{A.1}$$

where  $\dot{\epsilon}_1$  is the strain rate of the inner narrow portion,  $\dot{\epsilon}_{\Delta l_\theta}$  is the